The 2017 World Congress on
Advances in Structural Engineering and Mechanics (ASEM17)
28 August - 1 September, 2017, Ilsan(Seoul), Korea

Optimum Design of Multiple Tuned Mass Dampers for Vibration Suppression of Irregular Buildings

*Jie-Yong Jian[1)], Ging-Long Lin[2)] and Chi-Chang Lin[3)]

[1), 2),3)] *Department of Civil Engineering, National Chung Hsing University, Taichung 40227, Taiwan*
[1)] *pupuru88@gmail.com*

ABSTRACT

A multiple tuned mass damper (MTMD) system composed of multiple units of tuned mass damper (TMD) and arranged in parallel is proposed to reduce the vibration of torsionally-coupled buildings due to environmental loadings like wind and earthquake. By attaching MTMD to a structure, the structural vibration energy can be transferred to the MTMD and dissipated via the damping mechanism. Compared with the conventional single TMD, the proposed MTMD system is more effective and robust in mitigating frequency detuning effect.

This study deals with some practical design considerations such as the optimum location, moving direction and number of the MTMD system for a high-rise building with torsion coupling (TC) behavior. The control effectiveness of the MTMD system for the controlled mode was evaluated. The commercial structural analysis software, i.e. ETABS, was first applied to generate the finite element model of the target building and to analyze its TC behavior. Then, the number and optimum location (in plane and in elevation) of the MTMD system was determined based on the mode shape of the controlled mode. The optimal parameters of the MTMD system were calculated by an automatic program, which was based on the optimal design procedures developed by the authors. In order to evaluate the MTMD's control performance, the dynamic responses of a building with MTMD were compared with those of the uncontrolled case under different excitations. The results show that the proposed MTMD system is effective in reducing the vibration of buildings with TC behavior.

[1)] Graduate Student
[2)] Postdoctoral research fellow
[3)] Distinguished Professor

1 INTRODUCTION

In the recent decades, vibration control of civil engineering structures using passive tuned mass dampers (TMD) has received much acceptance after numerous analytical and experimental verifications (Lin and Wang 2012). TMD is one kind of passive-type devices and can be incorporated into any structure with less interference compared with others passive energy dissipation devices. Since 1975, many TMDs have been successfully installed in high-rise buildings, observatory towers, building floors and pedestrian bridges against natural and man-made loadings.

A multiple tuned mass damper (MTMD) consists of multiple units of single-degree-of- freedom (SDOF) substructures arranged in parallel. This device creates a broader bandwidth (Lin et al. 2017) than that of a single TMD, and thus, the variation of the controlled structural frequency can be covered to overcome the detuning problem. The concept of MTMD was first proposed by Xu and Igusa 1992. Since then, numerous studies on the design approach and control efficiency have been carried out theoretically, such as the dynamic and the design points of view studied MTMD (Abe and Fujino 1994), effectiveness of the MTMD system (Kareem and Kline 1996), dynamic characteristics of Structures with MTMD (Jangid 1995; Jangid and Datta 1997), optimum parameters of MTMD (Li 2000, 2003; Li and Liu 2003; Said and Vasant 2015).

Because center of mass location and rigid center location is inconsistent in a real structure, and the structural plane with geometric symmetry only receive the one direction force of symmetry axis, still possible to cause the structure to produce both horizontal and twist direction displacements. Thus, consider irregular buildings optimal installed floor, planar position and moving direction of PTMDs, and also Wang and Lin 2005 consider the applicability of multiple tuned mass dampers (MTMD) on the vibration control of irregular buildings. He et al. 2014 investigated coupled vibration control of tuned mass damper in both horizontal and torsional direction. Gunay S. 2015 proposes bi-directional coupled tuned mass dampers (BiCTMDs) for the seismic response control of two-way asymmetric-plan buildings subjected to bi-directional ground motions. Daniel and Lavan 2014 presented a formal optimization methodology for the seismic retrofitting of 3D irregular structures. Furthermore, practical design considerations such as the limited stroke (Lin et al. 2012), soil-structure interaction (SSI) effect was also investigated by researchers (Wang and Lin 2005; Jabary and Madabhushi 2015).

Finite element model (FEM) is a popular tool for structural design and dynamics analysis (Tuan and Shang 2014). The commercial structural analysis software, i.e. ETABS, was first applied to generate the finite element model of the target building and to analyze its TC behavior. Following are the proposed standard operating procedures (SOP) for optimal design of MTMD system. (1) Determine the number and optimum location (in plane and in elevation) of the MTMD system based on the mode shape of the controlled mode. (2) Calculate MTMD system's optimal parameters by an automatic program, which was based on the optimal design procedures developed by the authors. (3) Comparing the dynamic responses of a building with and without MTMD system under different excitations. The simulation results show that the proposed MTMD system is effective in reducing the vibration of buildings with TC behavior.

2 BUILDING WITH MTMD SYSTEMS

The general torsionally coupled multistory buildings as shown in Fig. 1 have the following features: (1) the principal axes of resistance for all the stories are identically oriented, along the x and y-axes shown; (2) the centers of mass of the floors do not lie on a vertical axis; (3) centers of resistance of the stories do not lie on a vertical axis, either, i.e. the static eccentricities at each story are not equal; (4) all floors do not have the same radius of gyration r about the vertical axis through the center of mass; and (5) ratios of the three stiffness quantities—translational stiffness in x and y directions and torsional stiffnessfor any story are different.

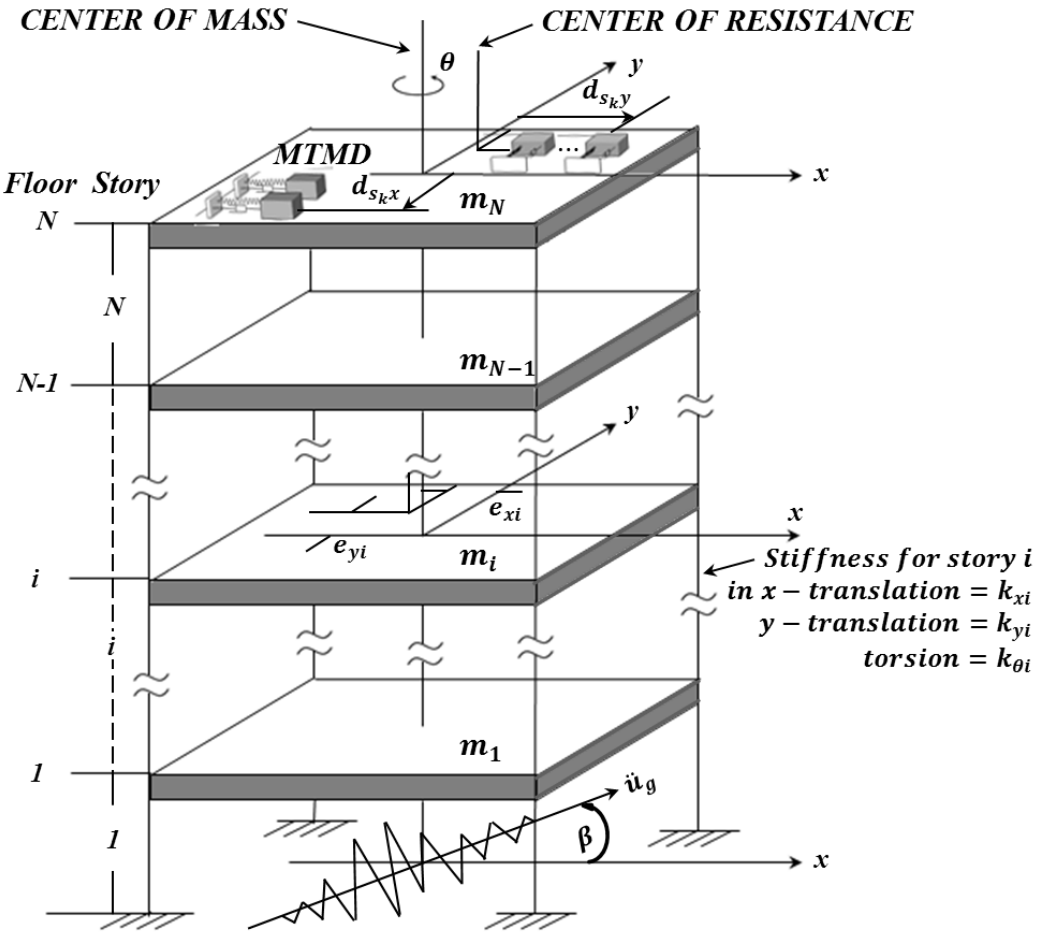

Fig. 1 N-story general torsionally coupled building MTMD system.

2.1 Dynamic equation of motion

Assume a MTMD with *p* TMD units installed at the *l*th floor of an 3*N*-degree-of-freedom (DOF) building structure and moving in y direction. The dynamic equation of motion of the combined MTMD system under earthquake excitation and external forces, can be written as

$$\mathbf{M}\ddot{\mathbf{u}}(t) + \mathbf{C}\dot{\mathbf{u}}(t) + \mathbf{K}\mathbf{u}(t) = \mathbf{M}_f\mathbf{r}\ddot{u}_g(t) + \mathbf{F}(t) \tag{1}$$

In Eq. (1)

$$\mathbf{u}(t) = \begin{bmatrix}\mathbf{u}_p(t)\\ \mathbf{v}_s(t)\end{bmatrix}, \mathbf{r} = \begin{bmatrix}\mathbf{r_p}\\ \mathbf{r_s}\end{bmatrix}, \mathbf{F}(t) = \begin{bmatrix}\mathbf{F_p}(t)\\ \mathbf{0}\end{bmatrix} \tag{2}$$

$\mathbf{u}_p(t) = [x_1 \quad y_1 \quad r_1\theta_1 \quad \cdots \quad x_i \quad y_i \quad r_i\theta_i \quad \cdots \quad x_N \quad y_N \quad r_N\theta_N] = 3N \times 1$ and $\mathbf{v}_s(t) = p \times 1$ dente the displacements of building relative to the ground and MTMD's displacement relative to the *i*th floor (called stroke). $\mathbf{r_p} = [-cos\beta \quad -sin\beta \quad 0 \quad \cdots \quad -cos\beta \quad -sin\beta \quad 0 \quad \cdots]$ is an $3N \times 1$ influence vector, and $\mathbf{r}_s$ is an $p \times 1$ influence vector with each element equal to $-sin\beta$. $\ddot{u}_g(t)$ represents the ground acceleration. $\mathbf{F}_p(t)$ is external forces acting on the structure.
Moreover, in Eq. (1)

$$\mathbf{M} = \begin{bmatrix}\mathbf{M}_p & \mathbf{0}\\ \mathbf{M}_{sp} & \mathbf{M}_s\end{bmatrix}, \quad \mathbf{C} = \begin{bmatrix}\mathbf{C}_p & \mathbf{C}_{ps}\\ \mathbf{0}^{\mathrm{T}} & \mathbf{C}_s\end{bmatrix}, \quad \mathbf{K} = \begin{bmatrix}\mathbf{K}_p & \mathbf{K}_{ps}\\ \mathbf{0}^{\mathrm{T}} & \mathbf{K}_s\end{bmatrix}, \quad \mathbf{M}_f = \begin{bmatrix}\mathbf{M}_p & \mathbf{0}\\ \mathbf{0}^{\mathrm{T}} & \mathbf{M}_s\end{bmatrix}$$

are (3*N*+*p*)×(3*N*+*p*) mass, damping and stiffness matrices of the combined system. $\mathbf{M}_P$, $\mathbf{C}_P$, and $\mathbf{K}_P$ are $3N \times 3N$ matrices of mass, damping and stiffness of the building, respectively. $\mathbf{M}_P = diag.(\mathbf{M}_1 \quad \mathbf{M}_2 \quad \cdots \quad \mathbf{M}_i \quad \cdots \quad \mathbf{M}_N) = 3N \times 3N$ mass matrix of building, $\mathbf{M}_i = diag.(m_i \quad m_i \quad I_i) = 3\times 3$ mass matrix, m_i is the lumped mass of floor *i*, I_i is the lumped rotational inertia of floor *i.* Similarly, $\mathbf{K} = 3N \times 3N$ stiffness matrix of building and expressed as

$$\mathbf{K}_p = \begin{bmatrix}
\mathbf{K}_{1,1} & \mathbf{K}_{1,2} & & & & & & \\
\mathbf{K}_{2,1} & \mathbf{K}_{2,2} & \mathbf{K}_{2,3} & & & & & \\
 & \mathbf{K}_{3,1} & \mathbf{K}_{3,2} & \mathbf{K}_{3,3} & & & & \\
 & & \cdot & \cdot & \cdot & & & \\
 & & & \mathbf{K}_{i,i-1} & \mathbf{K}_{i,i} & \mathbf{K}_{i,i+1} & & \\
 & & & & \cdot & \cdot & \cdot & \\
 & & & & & \mathbf{K}_{N-1,N-2} & \mathbf{K}_{N-1,N-1} & \mathbf{K}_{N-1,N} \\
 & & & & & & \mathbf{K}_{N,N-1} & \mathbf{K}_{N,N}
\end{bmatrix}$$

in which

$$\mathbf{K}_{i,i-1} = \begin{bmatrix}
-k_{x_i} & 0 & k_{x_i}\, e_{y_{i-1,i}}/r_{i-1} \\
0 & -k_{y_i} & k_{y_i}\, e_{x_{i-1,i}}/r_{i-1} \\
k_{x_i}\, e_{y_{i,i}}/r_i & -k_{y_i}\, e_{x_{i,i}}/r_i & (-k_{\theta_i} - k_{x_i} e_{y_{i,i}} e_{y_{i-1,i}} - k_{y_i} e_{x_{i,i}} e_{x_{i-1,i}})/r_{i-1} r_i
\end{bmatrix} \quad (i = 2 \sim N)$$

$$\mathbf{K}_{i,i} = \begin{bmatrix} k_{x_i} + k_{x_{i+1}} & 0 & (-k_{x_i} e_{y_{i,i}} - k_{x_{i+1}} e_{y_{i,i+1}})/r_i \\ 0 & k_{y_i} + k_{y_{i+1}} & k_{y_i} e_{x_{i,i}} + k_{y_{i+1}} e_{x_{i,i+1}}/r_i \\ (-k_{x_i} e_{y_{i,i}} - k_{x_{i+1}} e_{y_{i,i+1}})/r_i & (k_{y_i} e_{x_{i,i}} + k_{y_{i+1}} e_{x_{i,i+1}})/r_i & \begin{matrix}(k_{\theta_i} + k_{\theta_{i+1}} \\ +k_{x_i} e_{y_{i,i}}^2 + k_{x_{i+1}} e_{y_{i,i+1}}^2 \Big/ r_i^2 \\ +k_{y_i} e_{x_{i,i}}^2 + k_{y_{i+1}} e_{x_{i,i+1}}^2)\end{matrix} \end{bmatrix} \quad (i = 1 \sim N-1)$$

$$\mathbf{K}_{i,i} = \begin{bmatrix} k_{x_i} & 0 & -k_{x_i} e_{y_{i,i}}/r_i \\ 0 & k_{y_i} & k_{y_i} e_{x_{i,i}}/r_i \\ -k_{x_i} e_{y_{i,i}}/r_i & k_{y_i} e_{x_{i,i}}/r_i & (k_{\theta_i} + k_{x_i} e_{y_{i,i}}^2 + k_{y_i} e_{x_{i,i}}^2)/r_i^2 \end{bmatrix} \quad (i = N)$$

$$\mathbf{K}_{i,i+1} = \begin{bmatrix} -k_{x_{i+1}} & 0 & k_{x_{i+1}} e_{y_{i+1,i+1}}/r_{i+1} \\ 0 & -k_{y_{i+1}} & -k_{y_{i+1}} e_{x_{i+1,i+1}}/r_{i+1} \\ k_{x_{i+1}} e_{y_{i,i+1}}/r_i & -k_{y_{i+1}} e_{x_{i,i+1}}/r_i & \begin{matrix}(-k_{\theta_{i+1}} \\ -k_{x_{i+1}} e_{y_{i,i+1}} e_{y_{i+1,i+1}} \Big/ r_i r_{i+1} \\ -k_{y_{i+1}} e_{x_{i,i+1}} e_{x_{i+1,i+1}})\end{matrix} \end{bmatrix} \quad (i = 1 \sim N-1)$$

are the stiffness submatrices, where k_{x_i},k_{y_i} and k_{θ_i} are translational and rotational stiffnesses of story *i*; $e_{x_{i,i}}$ and $e_{x_{i,i+1}}$ denote the static eccentricites in *x*-axis at floor *i* with respect to story *i* and *i* + 1, respectively; and r_i is the radius of gyration of floor *i*. Assumed that $\mathbf{C}_p$ is a classical damping matrix.

Besides,

$$\mathbf{M}_s = diag.[m_{s_k}],\ \mathbf{C}_s = diag.[c_{s_k}],\ \mathbf{K}_s = diag.[k_{s_k}] \tag{3}$$

$$\mathbf{M}_{sp} = \mathbf{M}_s\mathbf{u},\ \mathbf{C}_{ps} = -(\mathbf{C}_s\mathbf{u})^{\mathrm{T}},\ \mathbf{K}_{ps} = -(\mathbf{K}_s\mathbf{u})^{\mathrm{T}} \tag{4}$$

where $\mathbf{M}_s$, $\mathbf{C}_s$, and $\mathbf{K}_s$ are $p \times p$ diagonal matrices and m_{s_k}, c_{s_k}, and k_{s_k} are mass, damping coefficient and stiffness coefficient of *k*th TMD ($k = 1, 2, \cdots, p$). In Eq. (4), $\mathbf{u} = \begin{bmatrix}\mathbf{0} & \mathbf{0} & \cdots & \mathbf{0}^{(3i-2)} & \mathbf{1}^{(3i-1)} & \boldsymbol{\upsilon}_{sy}{}^{(3i)} & \cdots & \mathbf{0}\end{bmatrix}$ is an $p \times 3N$ where $\mathbf{0}$, $\mathbf{1}$ and $\boldsymbol{\upsilon}_{sy}$ are $p \times 1$ vectors with each element equal to 0, 1 and $\upsilon_{sy} = d_{sy}/r_i$, respectively. The superscript (*i*) indicates the position of vector $\mathbf{0}$,$\mathbf{1}$ and $\boldsymbol{\upsilon}_{\mathbf{sy}}$ in matrix $\mathbf{u}$.

Assume $\mathbf{F}_{\boldsymbol{p}}(t) = \mathbf{0}$, let $\boldsymbol{\Phi}$ be the $3N \times 3N$ mode shape matrix of the building which obtained from the characteristic equation $\left[\mathbf{K}_{\mathrm{p}} - \omega_j^2 \mathbf{M}_{\mathrm{p}}\right]\boldsymbol{\phi}_j = 0$ for *j* modal and $\boldsymbol{\eta}(t)$ the

$3N \times 1$ modal displacement vector. Substuting $\mathbf{u}_p(\mathrm{t}) = \mathbf{\Phi\eta}(\mathrm{t})$ to Eq. (1) and premultiplying two sides of the building part by $\mathbf{\Phi}^T$, yields

$$\begin{bmatrix} \mathbf{M}_p^* & \mathbf{0} \\ \mathbf{M}_{sp}^* & \mathbf{M}_s^* \end{bmatrix} \begin{Bmatrix} \ddot{\boldsymbol{\eta}}(t) \\ \ddot{\mathbf{v}}_s(t) \end{Bmatrix} + \begin{bmatrix} \mathbf{C}_p^* & \mathbf{C}_{ps}^* \\ \mathbf{0}^{\mathrm{T}} & \mathbf{C}_s^* \end{bmatrix} \begin{Bmatrix} \dot{\boldsymbol{\eta}}(t) \\ \dot{\mathbf{v}}_s(t) \end{Bmatrix} + \begin{bmatrix} \mathbf{K}_p^* & \mathbf{K}_{ps}^* \\ \mathbf{0}^{\mathrm{T}} & \mathbf{K}_s^* \end{bmatrix} \begin{Bmatrix} \boldsymbol{\eta}(t) \\ \mathbf{v}_s(t) \end{Bmatrix} = \begin{bmatrix} \mathbf{\Gamma}_p \\ \mathbf{\Gamma}_s \end{bmatrix} \ddot{x}_g(t) \tag{5a}$$

where $\mathbf{M}_p^*$ and $\mathbf{M}_s^*$ are $3N \times 3N$ and $p \times p$ unity matrices, respectively, and

$$\mathbf{C}_p^* = diag.[2\xi_j\omega_j]; \mathbf{K}_p^* = diag.[\omega_j^2] \tag{5b, 5c}$$

$$\mathbf{C}_s^* = diag.[2\xi_{s_k}\omega_{s_k}]; \ \mathbf{K}_s^* = diag.[\omega_{s_k}^2] \tag{5d, 5e}$$

$$\mathbf{M}_{sp}^* = \begin{bmatrix} \phi_{3i-1,1} + \upsilon_{sy}\phi_{3i,1} & \phi_{3i-1,2} + \upsilon_{sy}\phi_{3i,2} & \cdots & \phi_{3i-1,3N} + \upsilon_{sy}\phi_{3i,3N} \\ \phi_{3i-1,1} + \upsilon_{sy}\phi_{3i,1} & \phi_{3i-1,2} + \upsilon_{sy}\phi_{3i,2} & \cdots & \phi_{3i-1,3N} + \upsilon_{sy}\phi_{3i,3N} \\ \vdots & \vdots & \ddots & \vdots \\ \phi_{3i-1,1} + \upsilon_{sy}\phi_{3i,1} & \phi_{3i-1,2} + \upsilon_{sy}\phi_{3i,2} & \cdots & \phi_{3i-1,3N} + \upsilon_{sy}\phi_{3i,3N} \end{bmatrix}_{p\times 3N} \tag{5f}$$

$$\mathbf{C}_{ps}^* = -\begin{bmatrix} C_{s_1}\mu_{s_1,1} & C_{s_2}\mu_{s_2,1} & \cdots & C_{s_p}\mu_{s_p,1} \\ C_{s_1}\mu_{s_1,2} & C_{s_2}\mu_{s_2,2} & \cdots & C_{s_p}\mu_{s_p,2} \\ \vdots & \vdots & \ddots & \vdots \\ C_{s_1}\mu_{s_1,3N} & C_{s_2}\mu_{s_2,3N} & \cdots & C_{s_p}\mu_{s_p,3N} \end{bmatrix}_{3N\times p} \tag{5g}$$

$$\mathbf{K}_{ps}^* = -\begin{bmatrix} K_{s_1}\mu_{s_1,1} & K_{s_2}\mu_{s_2,1} & \cdots & K_{s_p}\mu_{s_p,1} \\ K_{s_1}\mu_{s_1,2} & K_{s_2}\mu_{s_2,2} & \cdots & K_{s_p}\mu_{s_p,2} \\ \vdots & \vdots & \ddots & \vdots \\ K_{s_1}\mu_{s_1,3N} & K_{s_2}\mu_{s_2,3N} & \cdots & K_{s_p}\mu_{s_p,3N} \end{bmatrix}_{3N\times p} \tag{5h}$$

$$\mathbf{\Gamma}_p = \frac{\mathbf{\Phi}^{\mathrm{T}}\mathbf{M}_p\mathbf{r}}{\mathbf{\Phi}^{\mathrm{T}}\mathbf{M}_p\mathbf{\Phi}}; \ \mathbf{\Gamma}_s = -\mathbf{sin}\beta; \ \mathbf{\Phi}^{\mathrm{T}}\mathbf{M}_p\mathbf{\Phi} = diag[m_j^*]; \tag{5i,5j}$$

where ξ_j and ω_j are *j*th modal damping ratio and *j*th modal frequency of the building, respectively; ξ_{sk} and ω_{sk} are damping ratio and natural frequency of the *k*th TMD, respectively; $\boldsymbol{\mu}_s = \{\mu_{s_1,j} \ \ \mu_{s_2,j} \ \cdots \ \mu_{s_k,j} \ \cdots \ \mu_{s_p,j}\}$ where $\mu_{s_k,j} = (\phi_{3i-1,j} + \upsilon_{sy}\phi_{3i,j})\, m_{s_k}/m_j^*$ is mass ratio of the *k*th TMD to *j*th modal mass of the building; $m_j^* = \sum_{i=1}^{3N}\phi_{ij}^2 m_i$ *j*th generalized modal mass of the building; ϕ_{ij} is the *i*th value of the *j*th mode shape; and $\mathbf{\Gamma}_p$ is the modal participating vector with its *j*th value $\Gamma_{p,j} = (\sum_{i=1}^{3N}\phi_{ij}m_i)/m_j^*$.

2.2 Modal transfer function

In Eq. (5a), consider the *j*th mode of the building and take Fourier transform for both sides. The *j*th modal displacement vector of the building and the stroke vector of MTMD can be represented in frequency domain, in terms of transfer function, as

$$\begin{Bmatrix} \eta_j(\omega) \\ \mathbf{V}_s(\omega) \end{Bmatrix} = \mathbf{A}^{-1} \begin{bmatrix} \Gamma_{p_j} \\ \mathbf{\Gamma}_s \end{bmatrix} \ddot{X}_g(\omega) = \begin{bmatrix} H_{pp_j}(\omega) & \mathbf{H}_{ps}(\omega) \\ \mathbf{H}_{sp}(\omega) & \mathbf{H}_{ss}(\omega) \end{bmatrix} \begin{bmatrix} \mathbf{\Gamma}_{p_j} \\ \mathbf{\Gamma}_s \end{bmatrix} \ddot{X}_g(\omega) \tag{6}$$

In detail,

$$\begin{Bmatrix} \eta_j(\omega) \\ \hdashline v_{s_1}(\omega) \\ v_{s_2}(\omega) \\ \vdots \\ v_{s_k}(\omega) \\ \vdots \\ v_{s_p}(\omega) \end{Bmatrix} = \left[\begin{array}{c:cccccc} A_j & C_1 & C_2 & \cdots & C_k & \cdots & C_p \\ \hdashline D_1 & B_1 & 0 & \cdots & 0 & \cdots & 0 \\ D_2 & 0 & B_2 & & & & 0 \\ \vdots & \vdots & & \ddots & & & \vdots \\ D_k & 0 & & & B_k & & 0 \\ \vdots & \vdots & & & & \ddots & \vdots \\ D_p & 0 & 0 & \cdots & 0 & \cdots & B_p \end{array}\right]^{-1} \begin{Bmatrix} \Gamma_{p_j} \\ \hdashline \Gamma_{s_1} \\ \Gamma_{s_2} \\ \vdots \\ \Gamma_{s_k} \\ \vdots \\ \Gamma_{s_p} \end{Bmatrix} \ddot{X}_g(\omega) \tag{7}$$

where

$$A_j = -\omega^2 + i\omega(2\xi_j\omega_j) + \omega_j^2 \quad ; \quad B_k = -\omega^2 + i\omega(2\xi_{s_k}\omega_{s_k}) + \omega_{s_k}^2$$
$$C_k = \mu_{s_k,j}[-i\omega(2\xi_{s_k}\omega_{s_k}) - \omega_{s_k}^2] \quad ; \quad D_k = -\omega^2(\phi_{3l-1,j} + \upsilon_{sy}\phi_{3l,j})$$
$$k = 1, 2, \ldots, p$$

The inverse of matrix in Eq. (7) can be solved either numerically or analytically and Eq. (6) can be rewritten as

$$\begin{Bmatrix} \eta_j(\omega) \\ \hdashline v_{s_1}(\omega) \\ v_{s_2}(\omega) \\ \vdots \\ v_{s_k}(\omega) \\ \vdots \\ v_{s_p}(\omega) \end{Bmatrix} = \begin{bmatrix} H_{1,1} & H_{1,2} & H_{1,3} & \cdots & H_{1,k} & \cdots & H_{1,p+1} \\ H_{2,1} & H_{2,2} & H_{2,3} & \cdots & H_{2,k} & \cdots & H_{2,p+1} \\ H_{3,1} & H_{3,2} & H_{3,3} & \cdots & & \cdots & H_{3,p+1} \\ \vdots & \vdots & \vdots & \ddots & & & \vdots \\ H_{k,1} & H_{k,2} & & & H_{k,k} & & H_{k,p+1} \\ \vdots & \vdots & \vdots & & & \ddots & \vdots \\ H_{p+1,1} & H_{p+1,2} & H_{p+1,3} & \cdots & H_{p+1,k} & \cdots & H_{p+1,p+1} \end{bmatrix} \begin{Bmatrix} \Gamma_{p_j} \\ \hdashline \Gamma_{s_1} \\ \Gamma_{s_2} \\ \vdots \\ \Gamma_{s_k} \\ \vdots \\ \Gamma_{s_p} \end{Bmatrix} \ddot{X}_g(\omega) \tag{8}$$

From Eq. (8), the *j*th modal displacement of the building and the *k*th TMD stroke of the MTMD can be expressed as

$$\eta_j(\omega) = \left[H_{11}(\omega)\Gamma_{p_j} + \sum_{l=1}^{p} H_{1,l+1}(\omega)\Gamma_{s_l} \right] \ddot{X}_g(\omega) = H_{\eta_j \ddot{X}_g}(\omega)\ddot{X}_g(\omega) \tag{9a}$$

$$v_{s_k}(\omega) = [H_{k1}(\omega)\Gamma_{p_j} + \sum_{l=1}^{p} H_{k,l+1}(\omega)\Gamma_{s_l}]\ddot{X}_g(\omega) = H_{v_{sk}\ddot{X}_g}(\omega)\ddot{X}_g(\omega) \quad (9b)$$

It is noticeable that $\eta_j(\omega)$ represents the modified *j*th modal-displacement of the building with the existence of MTMD, not the *j*th modal displacement of the building-MTMD system.

2.3 Optimization design of MTMD

In this study, a MTMD group is assigned to control single structural vibration mode due to ground motions. For the evaluation of MTMD control effectiveness, the mean-squared response ratio of *j*th structural mode with MTMD to that without MTMD is defined as the performance index. In usual, white-noise excitation is chosen as representative of earthquakes in design stage because of uncertain ground motion. In fact, according to Lin et al. 2001, the control performance of a TMD has no considerable difference between Kanai-Tajimi filtered noise and white-noise excitations. Therefore, the MTMD performance index can be written as

$$R_j = \frac{E[\eta_j^2]_{\text{with MTMD}}}{E[\eta_j^2]_{\text{w/o MTMD}}} = \frac{\int_{-\infty}^{\infty} |H_{\eta_j \ddot{X}_g}(\omega)|^2_{\text{with MTMD}}\, d\omega}{\int_{-\infty}^{\infty} |H_{\eta_j \ddot{X}_g}(\omega)|^2_{\text{w/o MTMD}}\, d\omega} \quad (10)$$

It can be derived that R_j is a function of ξ_j, ϕ_j (structural parameters), $\mu_{s_k,j}, \xi_{s_k}$, and γ_{f_k} where *k* =1, 2, …, *p* (MTMD's parameters) and is independent of ω_j. $\gamma_{f_k} = \omega_{s_k}/\omega_j$ is the ratio of frequency of the *k*th TMD unit to the *j*th modal frequency of the building. Note that there are 3*p* unknown MTMD parameters with a given entire mass of the MTMD.

In practice, the most economical MTMD layout is to design each TMD unit with an identical stiffness coefficient, k_{s_o}, and identical damping coefficient, c_{s_o}, especially when the number of TMD unit increases. This layout can reduce the cost of making new molds. It can be derived that

$$k_{s_0} = \frac{m_{s_t}}{\sum_{k=1}^{p} \frac{1}{\omega_j^2 r_{f_k}^2}}, \quad c_{s_0} = \frac{2\xi_{s_k}}{r_{f_k}\omega_j} k_{s_0}, \quad m_{s_k} = \frac{k_{s_0}}{r_{f_k}^2 \omega_j^2} \quad (11)$$

where $m_{s_t} = \sum_{k=1}^{p} m_{s_k}$ is the total mass of MTMD. Based on Eq.(11), the *p* number of TMD's damping ratios, $\xi_{s_1}, \xi_{s_2}, \cdots, \xi_{s_k}, \cdots, \xi_{s_p}$, can be related to one variable ξ_{s_0} because $\xi_{s_k} = \xi_{s_0} r_{f_k}$. Moreover, with the total mass ratio of MTMD $\mu_{s_t,j} = (\phi_{3i-1,j} + v_{sy}\phi_{3i,j})m_{s_t}/m_j^*$ assigned in prior, the modal mass ratio of the *k*th TMD unit can be calculated as

$$\mu_{s_k,j} = \mu_{s_t,j} \frac{1/r_{f_k}^2}{\sum_{l=1}^{p} 1/r_{f_l}^2} \quad (12)$$

Without any restriction on the frequency distribution of TMD units, the optimization of MTMD with identical stiffness and damping coefficient involves (p + 1) independent parameters, $\gamma_{f_1}, \gamma_{f_2}, \cdots, \gamma_{f_k}, \cdots, \gamma_{f_p}$ and ξ_{s_0}. Theoretically, with given values of ω_j, ξ_j and ϕ_{ij}, the optimal MTMD parameters, $(\gamma_{f_1})_{opt}$, $(\gamma_{f_2})_{opt}, \cdots (\gamma_{f_p})_{opt}$ and $(\xi_{s_0})_{opt}$, can be obtained by solving the following equation system which is established by differentiating R_j with respect to the (p + 1) parameters and equating to zero, respectively, to minimize R_j.

$$\frac{\partial R_j}{\partial r_{f_1}} = 0, \quad \frac{\partial R_j}{\partial r_{f_2}} = 0, \ldots, \quad \frac{\partial R_j}{\partial r_{f_p}} = 0, \quad \frac{\partial R_j}{\partial \xi_{s_0}} = 0 \tag{13}$$

Then, the optimum stiffness, $(k_{s_0})_{opt}$, optimum damping, $(c_{s_0})_{opt}$, and optimum mass for kth TMD unit, $(m_{s_k})_{opt}$, can be calculated by Eqs. (11). However, the optimization process is usually performed by numerical searching techniques which can be found in mathematical software packages, such as MATLAB.

3 DESIGN MTMD CONCEPT

For a torsionally coupled shear building, the first three modes are the most important to the translational and torsional responses of each floor. However, the translations in x and y directions have different dominant modes. With FEM (finite element method) model of ETABS, we can find out the structural properties by modal parameters. For a torsionally coupled building optimal location has been shown by Wang and Lin 2005. Thus, In Eq. (5), the optimum installation floor and planar position of MTMD can be determined by maximizing $\left|\phi_{3i-1,j} + v_{sy}\phi_{3i,j}\right|$ for moving in y direction, maximizing $\left|\phi_{3i-2,j} + v_{sx}\phi_{3i,j}\right|$ for moving in x direction. Finally, a SOP (standing operating procedures) was proposed for designing MTMD's optimal parameters as showed in Fig. 2.

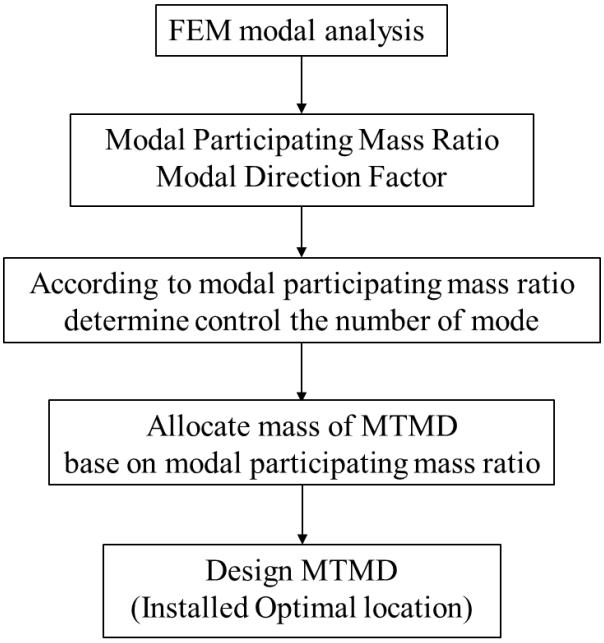

Fig. 2 Design SOP

Step (1): Modal analysis by using FEM model
Step (2): Compute modal participating mass ratio (MPMR) and modal direction factor (MDF) based on the modal parameters. The MPMR values indicate the dominant modes in each direction while the MDF values indicate whether the concerned mode including torsion effect or not.
Step (3): The modes to be controlled are determined based on the MPMR values. (In this study, the sum of MPMR values of the controlled modes reaches 85% of the sum of all MPMR values).
Step (4): The total mass of each MTMD system for each controlled mode is assigned based on the proportion of the MPMR value in each mode.
Step (5): Optimal MTMD's parameters are calculated by an automatic program.

4 NUMERICAL VERIFICATIONS

Two FEM models developed by ETABS are showed in Fig. 3 and Fig. 4. Both of them are 5 stories buildings. Building (B1) is a symmetrical structure. Weak direction is y. Table 1 and Table 2 list the MPMS and MDF values computed by modal parameters of building B1, it is seen the mode order is $y - x - \theta$. After adding bracings in two sides of building (B1), the building (B2), becomes a torsionally coupled building. Table 3 and Table 4 list its the MPMS and MDF values. The total mass ratio of the MTMD systems is 1% in the following numerical examples.

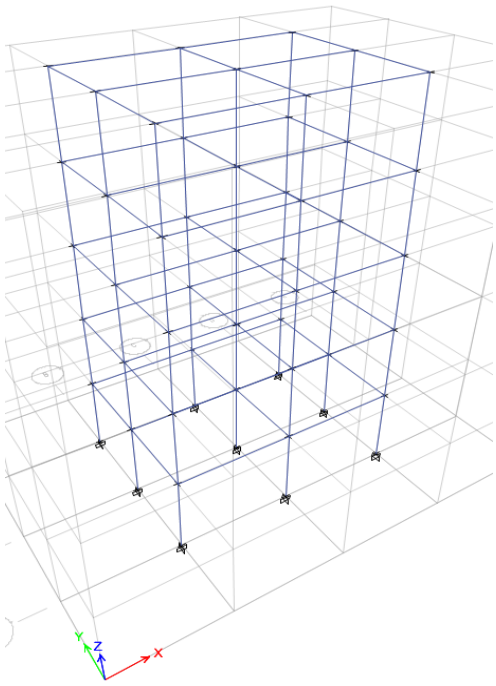

Fig. 3 B1 FEM model

Table 1 B1 Modal Participating Mass Ratios

Mode	Period (Sec)	*x*	*y*	*θ*
1	0.55	0	0.88	0
2	0.463	0.88	0	0
3	0.439	0	0	0.88
4	0.19	0	0.08	0
5	0.16	0.08	0	0

Table 2 B1 Modal Direction Factor

Mode	Period (Sec)	*x*	*y*	*θ*
1	0.55	0	1	0
2	0.463	1	0	0
3	0.439	0	0	1
4	0.19	0	1	0
5	0.16	1	0	0

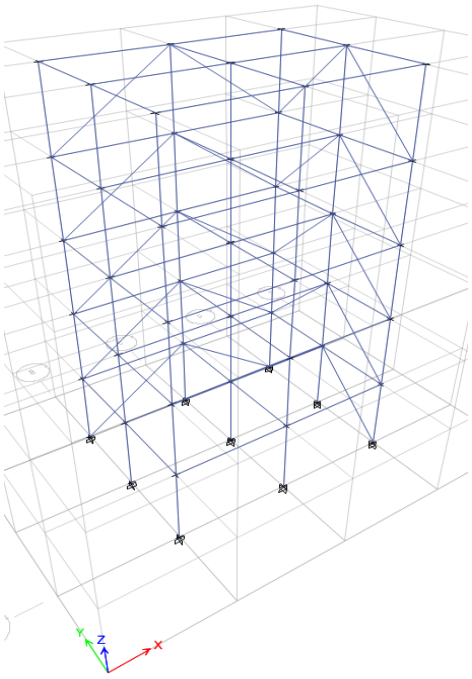

Fig 4. B2 FEM model

Table 3 B2 Modal Participating Mass Ratios

Mode	Period (Sec)	*x*	*y*	*θ*
1	0.49	0.09	0.58	0.22
2	0.38	0.45	0.27	0.17
3	0.28	0.34	0.04	0.50
4	0.17	0.01	0.06	0.02
5	0.13	0.04	0.03	0.02

Table 4 B2 Modal Direction Factor

Mode	Period (Sec)	*x*	*y*	*θ*
1	0.49	0.11	0.65	0.24
2	0.38	0.51	0.30	0.19
3	0.28	0.39	0.04	0.57
4	0.17	0.11	0.65	0.24
5	0.13	0.51	0.30	0.19

4.1 Design MTMD

Firstly, according to the MPMR values of B1 building, two groups of MTMD systems are designed to control 1st mode (Y direction) and the 2nd mode (X direction) based on the proposed SOP. The sum of MPMR values (in Y direction) of the controlled two modes is 88%. From the MDF values of building B1, it is found the first two modes are pure translation modes. Therefore, the two groups of MTMD systems are installed in the center of mass (5F) show in Fig. 5. Table 5 lists the system parameters of the two MTMD systems. Second, according to the MPMR values of building B2, three groups of MTMD systems are designed to control the 1st mode (Y direction), the 2nd mode (X direction) and the 3rd mode (X direction). From MDF values of building B2, it is found the first three modes are all torsional coupled. Therefore, three groups of MTMD systems are installed in the optimal location showed in Fig. 6. The sum of MPMR values of the controlled three modes of in X and Y direction are larger than 85%. Table 6 lists the system parameters of the three groups of MTMD systems. Total mass ratio is taken to be 1%. Mass ratio of each MTMD group is assigned based on the proportion of MPMR values.

Table 5 MTMD parameters for controlling 1st and 2nd modes (B1 building)

Control 1st mode				
Mass ratio	Mass (ton)		Stiffness (KN/m)	Damping (KN-s/m)
0.5 %	TMD 1	0.73	85.25	0.34
	TMD 2	0.66		
	TMD 3	0.61		

Control 2nd mode				
Mass ratio	Mass (ton)		Stiffness (KN/m)	Damping (KN-s/m)
0.5 %	TMD 1	0.73	120.30	0.40
	TMD 2	0.66		
	TMD 3	0.61		

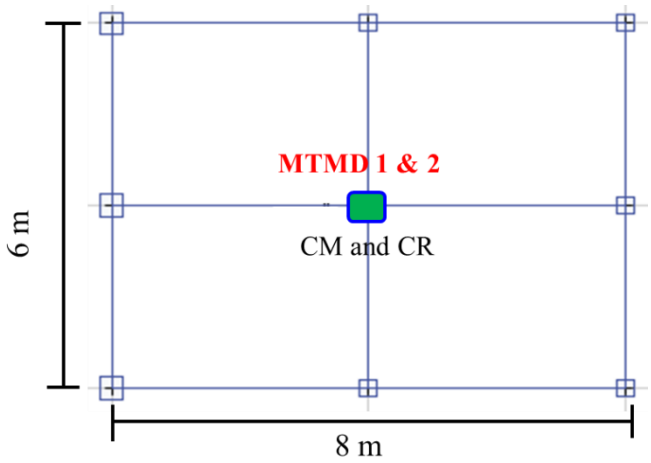

Fig. 5 Location of each group of MTMD system on 5F (B1 building)

Table 6 MTMD parameters for controlling 1st, 2nd and 3rd modes (B2 building)

Control 1st mode				
Mass ratio.	Mass (ton)		Stiffness (KN/m)	Damping (KN-s/m)
0.42 %	TMD 1	0.67	87.22	0.63
	TMD 2	0.55		
	TMD 3	0.46		

Control 2nd mode				
Mass ratio.	Mass (ton)		Stiffness (KN/m)	Damping (KN-s/m)
0.33 %	TMD 1	0.50	116.91	0.43
	TMD 2	0.43		
	TMD 3	0.38		

Control 3rd mode				
Mass ratio.	Mass (ton)		Stiffness (KN/m)	Damping (KN-s/m)
0.25 %	TMD 1	0.37	163.17	0.40
	TMD 2	0.33		
	TMD 3	0.30		

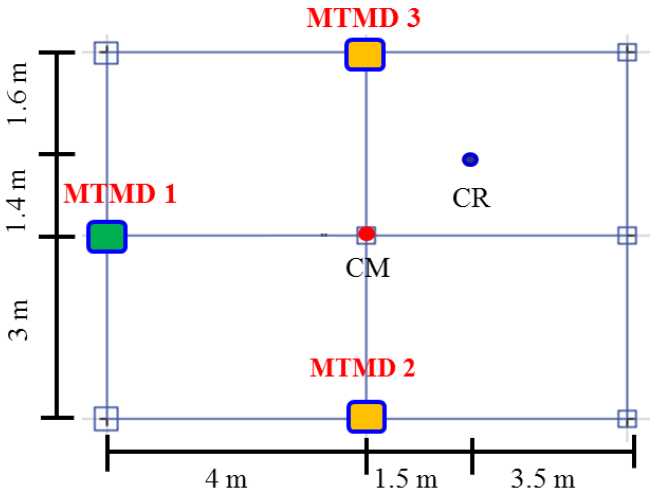

Fig. 6 Location of each group of MTMD system on 5F (B2 building)

4.2 Frequency domain analysis

Through ETABS analysis, assume that the seismic force is white noise. Fig. 7 depicts the transfer functions of acceleration w/ and w/o MTMD for x direction and y direction of B1 top floor center of mass from $\beta = 0^{\circ}$ and $\beta = 90^{\circ}$. Fig. 8 and Fig. 9 depicts the transfer functions of acceleration for x direction and y direction of B2 the

lower left corner of top floor from $\beta = 0^{\circ}$ and $\beta = 90^{\circ}$. At two angles, it is found that mode amplitude is reduced in both directional responses of B1 and B2.

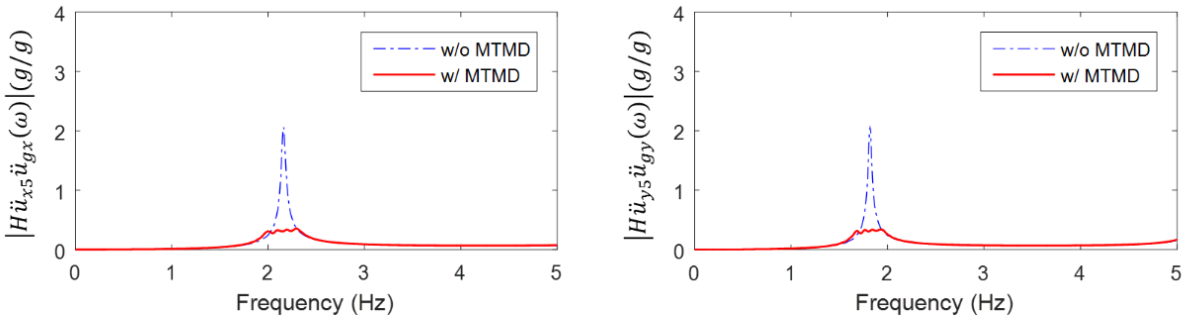

Fig. 7 B1 building top floor acceleration (C.M.) transfer functions for x direction as $\beta = 0^{\circ}$ (left) and y direction as $\beta = 90^{\circ}$ (right)

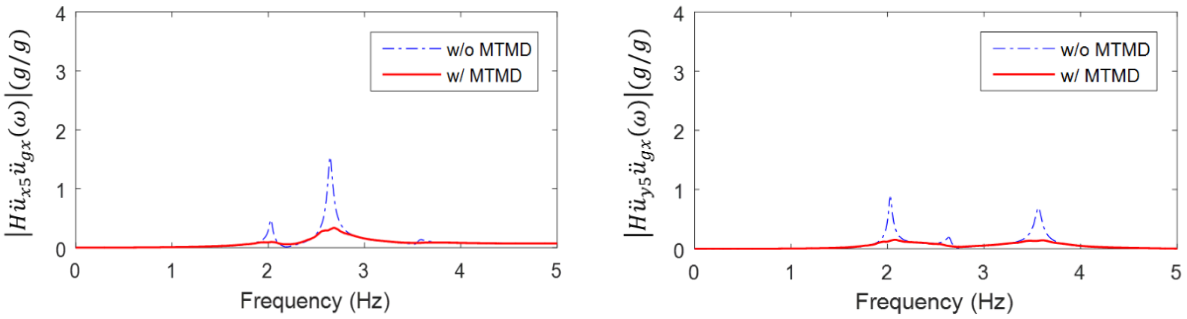

Fig. 8 B2 building top floor acceleration (lower left corner) transfer functions for x direction (left) and y direction (right) as $\beta = 0^{\circ}$

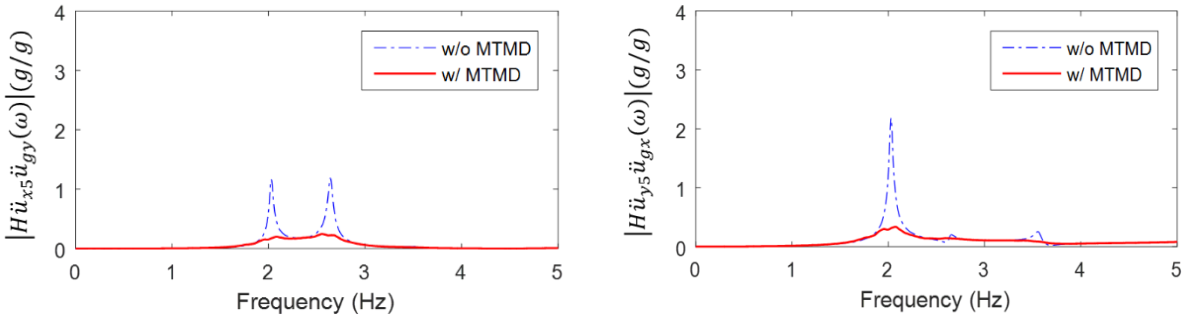

Fig. 9 B2 building top floor acceleration (lower left corner) transfer functions for x direction (left) and y direction (right) as $\beta = 90^{\circ}$

4.3 Time domain analysis

Further, input real earthquake, i.e. El Centro (1940) from $\beta = 90^{\circ}$ and $\beta = 0^{\circ}$. Fig. 10 depicts the time history acceleration responses w/ and w/o MTMD for y direction and x direction of B1 top floor center of mass. Fig. 11 and Fig. 12 depicts the time history acceleration responses w/ and w/o MTMD for y direction and x direction of B2 the lower

left corner of top floor. Identically, root-mean-square responses are reduced show in Table 7. MTMD system is effective in reducing the vibration of symmetrical building and building with TC behavior.

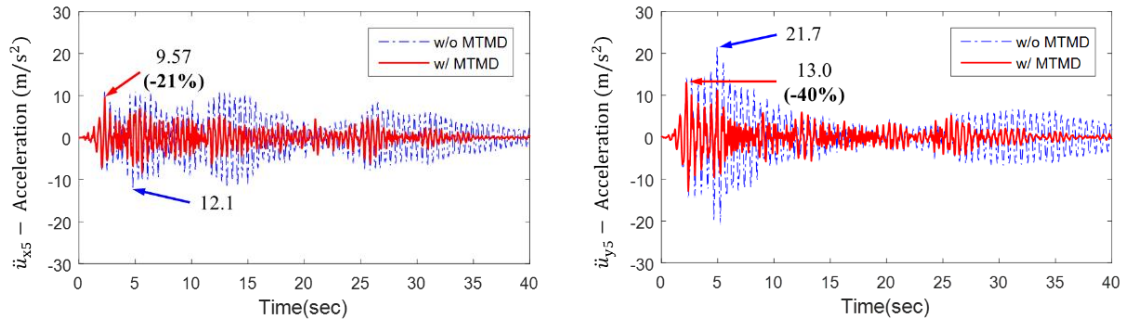

Fig. 10 B1 building top floor acceleration (C.M.) time history for x direction as $\beta = 0^{\circ}$ (left) and y direction as $\beta = 90^{\circ}$ (right)

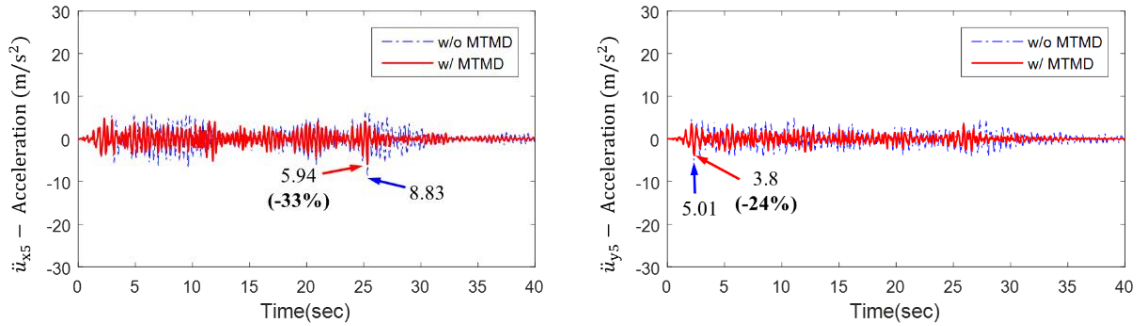

Fig. 11 B2 building top floor acceleration (lower left corner) time history for x direction (left) and y direction (right) as $\beta = 0^{\circ}$

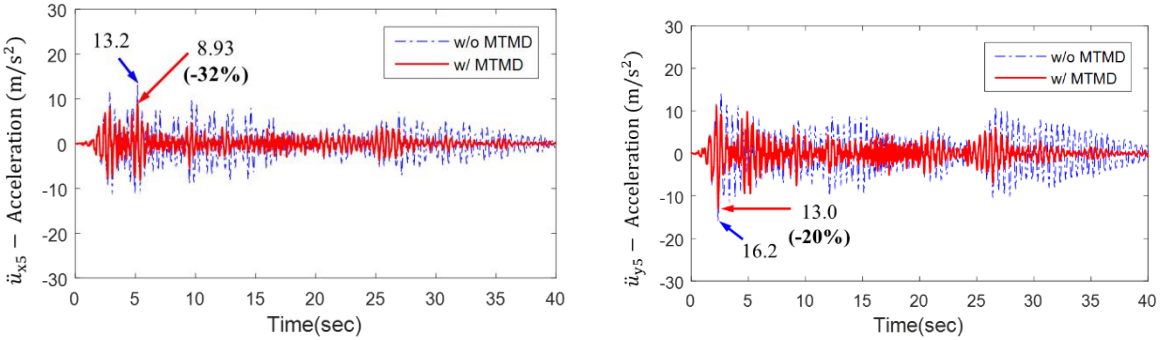

Fig. 12 B2 building of top floor acceleration (lower left corner) time history for x direction (left) and y direction (right) as $\beta = 90^{\circ}$

Table 7 Control performance of MTMD under El Centro (1940)

Case	β	Direction	Location	RMS acceleration (m/s^2)	
				w/o	w/MTMD
B1	0°	x	CM	3.79	1.70 (-55%)
	90°	y		4.27	2.01 (-53%)
B2	0°	x	lower left corner	1.87	1.15 (-38%)
		y		1.36	0.79 (-42%)
	90°	x		2.77	1.35 (-51%)
		y		3.71	1.92 (-48%)

5. CONCLUSIONS

This study deals with theoretical derivation and practical design considerations for optimal design of a MTMD system. The commercial structural analysis software was first applied to generate the finite element model of the target building and to analyze its TC behavior. Then, a standard operating procedures for optimal design of MTMD system was proposed as followings: (1) Determine the number and optimum location (in plane and in elevation) of the MTMD system based on the mode shape of the controlled mode. (2) Calculate MTMD system's optimal parameters by an automatic program, which was based on the optimal design procedures developed by the authors. (3) Comparing the dynamic responses of a building with and without MTMD system under different excitations. The simulation results show the proposed optimal MTMD system is effective in reducing the vibration of buildings with TC behavior. Therefore, the accuracy of theoretical derivation and the automatic program were verified.

REFERENCES

Abe, M., and Fujino, Y. (1994), "Dynamic characterization of multiple tuned mass dampers and some design formulas." *Earthq. Eng. Struct. Dyn*., **23**(8), 813–835.

Daniel, Y., and Lavan, O. (2014), "Gradient based optimal seismic retrofitting of 3D irregular buildings using multiple tuned mass dampers." *Comput. Struct*., **139**, 84–97.

Said, E. and Vasant, M. (2015), "Optimum tuned mass damper for wind and earthquake response control of high-rise building." *Adv. Struct. Eng*., New Delhi: Springer India, 1475–1487.

Gunay S., M. M. (2015), "Measuring bias in structural response caused by ground motion scaling." *Int. Assoc. Earthq. Eng*., **44**, 657–675.

He, H. X., Han, E. Z., and Lv, Y. W. (2014), "Coupled Vibration Control of Tuned Mass Damper in Both Horizontal and Torsional Direction." *Appl. Mech. Mater*., 578–579, 1000–1006.

Jabary, R. N., and Madabhushi, S. P. G. (2015), “Tuned mass damper effects on the response of multi-storied structures observed in geotechnical centrifuge tests.” *Soil Dyn. Earthq. Eng*., **77**, 373–380.

Jangid, R. S. (1995), “Dynamic characteristics of structures with multiple tuned mass dampers.” *Struct. Eng. Mech*., **3**(5), 497–509.

Jangid, S. R., andDatta, T. K. (1997), “Performance of multiple tuned mass dampers for torsionally coupled system.” *Earthq. Eng. Struct. Dyn*., **26**(3), 307–317.

Kareem, A., andKline, S. (1996), “Performance of Multiple Mass Dampers under Random Loading.” *J. Struct. Eng*., **122**(8), 981–982.

Li, C. (2000), “Performance of multiple tuned mass dampers for attenuating undesirable oscillations of structures under the ground acceleration.” *Earthq. Eng. Struct. Dyn*., **29**(9), 1405–1421.

Li, C. (2003), “Multiple active-passive tuned mass dampers for structures under the ground acceleration.” *Earthq. Eng. Struct. Dyn*., **32**(6), 949–964.

Li, C., and Liu, Y. (2003), “Optimum multiple tuned mass dampers for structures under the ground acceleration based on the uniform distribution of system parameters.” *Earthq. Eng. Struct. Dyn*., **32**(5), 671–690.

Lin, C.C. and Wang, J.F. (2012), *Optimal Design and Practical Considerations of Tuned Mass Dampers for Structural Control*, Chapter 6 of Design Optimization of Active and Passive Structural Control Systems, IGI Global Publisher, USA.

Lin, C.C., Wang, J.F., Lien, C.H., Chiang, H.W., & Lin, C.S. (2010), "Optimum design and experimental study of multiple tuned mass dampers with limited stroke." *Earthq. Eng. Struct. Dyn*., **39**, 1631-1651.

Lin, C.C., Lin, G.L., and Chiu, K.C. (2017), “Robust design strategy for multiple tuned mass dampers with consideration of frequency bandwidth.” *Int. J. Struct. Stab. Dyn*., **17**(1), 1750002.

Tuan, A.Y., andShang, G.Q. (2014), “Vibration control in a 101-storey building using a tuned mass damper.” *Journal of Applied Science and Engineering*, **17**(2), 141–156.

Wang, J.F., and Lin, C.C. (2005), “Seismic performance of multiple tuned mass dampers for soil–irregular building interaction systems.” *Int. J. Solids Struct*., **42**(20), 5536–5554.

Xu, K., and Igusa, T. (1992), “Dynamic characteristics of multiple substructures with closely spaced frequencies.” *Earthq. Eng. Struct. Dyn*., **21**(12), 1059–1070.